

Supporting Information

**The Strongest Size: Size-Dependent Elastic Strength in PbS Nanocrystals**

*Kaifu Bian,<sup>a</sup> William Bassett,<sup>b</sup> Zhongwu Wang,<sup>c</sup> Tobias Hanrath,<sup>a\*</sup>*

<sup>a</sup>School of Chemical and Biomolecular Engineering, <sup>b</sup>Department of Earth and Atmospheric Sciences, <sup>c</sup>Cornell High Energy Synchrotron Source (CHESS), Cornell University, Ithaca, NY, 14853

\*Corresponding Author: Tobias Hanrath, th358@cornell.edu

<b>1. Experimental Methods.....</b>	<b>1</b>
<b>2. WAXS Measurements .....</b>	<b>3</b>
<b>3. Calculation of Bulk Modulus .....</b>	<b>3</b>

---

---

## 1. Experimental Methods

### a. Synthesis of PbS Nanocrystals

PbS nanocrystals (NCs) used in this study were prepared using the method reported by Hines and Scholes<sup>1</sup>. In a typical synthesis, 0.45 g of lead oxide powder was mixed with 20 mL of oleic acid. Then the solution was heated to 150 °C for one hour under nitrogen flow to form a lead oleate solution and degas. The solution was then cooled down or further heated up to injection temperature ranging from 90 to 200°C. The injection temperature determines the size of synthesized NCs. In a nitrogen glovebox, 210  $\mu$ L of bis(trimethylsilyl)sulfide was dissolved in 10 mL of 1-octadecene, stirred thoroughly and then injected rapidly into the vigorously stirred lead oleate solution. Immediate formation of PbS NCs was indicated by color change of the mixture from transparent to dark. NCs were collected after reaction for 1 min then washed twice by sequential precipitation with ethanol and redispersion in hexane. Finally the solvent was removed by nitrogen flow and dry NCs were stored inside a nitrogen glovebox (oxygen <1 ppm).

### b. Transmission Electron Microscopy for NC Size Measurements

Dilute hexane solution of PbS NC samples were dropped on carbon coated copper grids for transmission electron microscopy (TEM) imaging. TEM images were taken using a FEI Tecnai T-12 microscope operated at 120 kV. The average diameter of NCs is determined by statistics on at least 200 NCs in multiple TEM images. Figure S1 shows representative TEM images and corresponding diameter histograms of the six samples involved in this study. The sizes of the PbS NCs are determined to be  $3.0\pm0.3$ ,  $3.7\pm0.3$ ,  $6.7\pm0.6$ ,  $8.5\pm0.8$ ,  $11.3\pm0.9$  and  $16.1\pm1.9$  nm in diameter  $D_0$ .

### c. In-situ High-Pressure X-ray Scattering Measurements.

High pressure was generated by a diamond anvil cell (DAC) consisting of two aligned diamond anvils (Figure 1). Saturated toluene suspension of PbS NCs was loaded into a 150- $\mu$ m diameter hole in a pre-indented stainless-steel gasket and then encapsulated and pressurized by the diamond anvils up to 6 GPa. Toluene served as both solvent and pressure media to decouple inter-NC interactions and provide hydrostatic pressure. Multiple ruby chips were placed in the DAC with the sample to measure pressure using standard ruby fluorescence method. The pressure gradient within the sample chamber never exceeded 0.2 GPa in all measurements.

X-ray scattering measurements were performed at the B1 beamline at Cornell High Energy Synchrotron Source (CHESS). Monochromatic x-ray of wavelength of 0.4859 Å was generated by two Ge (111) single crystals. Then the beam size was reduced to 100  $\mu$ m by a collimator. Wide-angle x-ray scattering (WAXS) patterns were collected by a large-area Mar345 image plate detector (Figure 1). The sample-to-detector distance was calibrated using a CeO<sub>2</sub> standard to 847.8 mm. The scattering patterns were then integrated by Fit2D software<sup>2</sup> and analyzed.

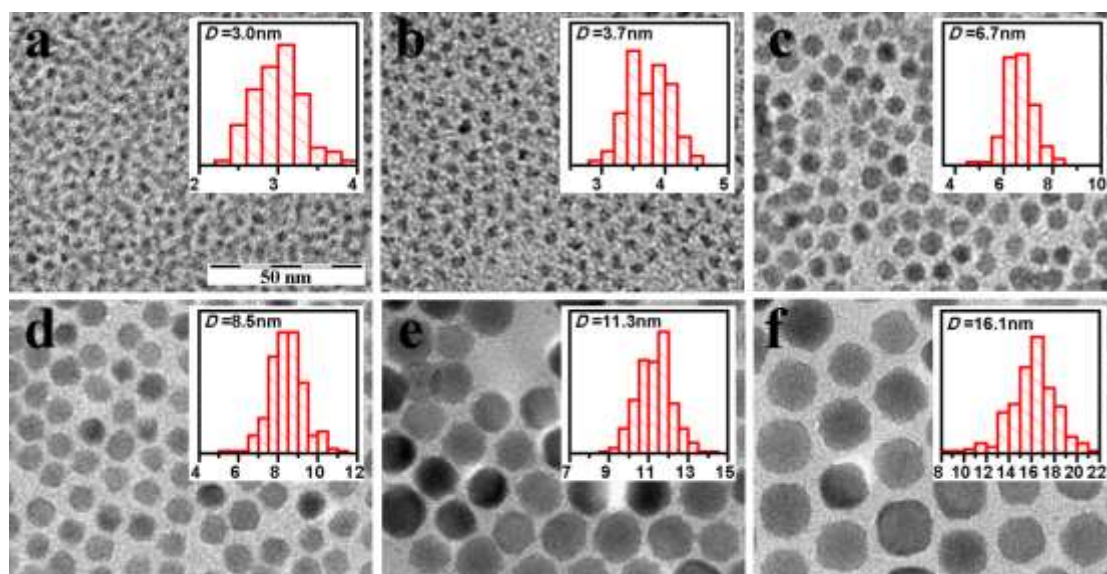


**Figure S1.** TEM images of (a) 3.0, (b) 3.7, (c) 6.7, (d) 8.5, (e) 11.3 and (f) 16.1 nm PbS NCs. Insets shows corresponding histogram of NQD diameter by counting at least 200 NQDs.

## 2. WAXS Measurements

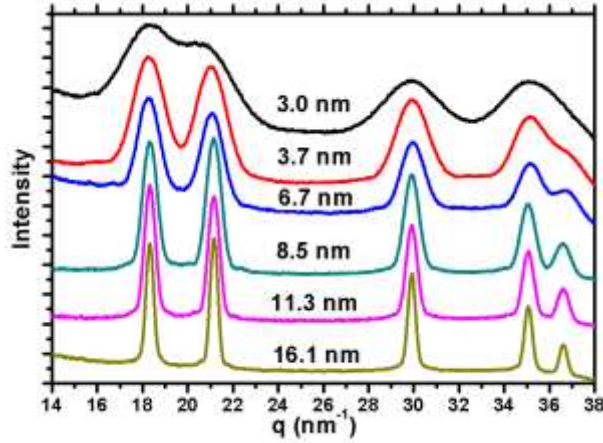


**Figure S2.** WAXS patterns of PbS NCs samples under ambient conditions

Figure S2 shows the WAXS patterns of the six PbS NC samples under ambient pressure confirming rock salt crystal structure. The scattering peaks broaden as NC size decreases due to size-dependent Scherrer broadening effect. The peak positions were determined by fitting them to Gaussian peaks. Lattice parameters were calculated by eqn. S1. Then the ambient lattice constant  $a_0$  as in Table 1 was obtained from  $d_{hkl}$  by the software UnitCell.<sup>3</sup> The 95% confidence interval is  $\sim 0.001 \text{ \AA}$  in all case.

$$d_{hkl} = 2\pi / q_{hkl} \quad (\text{S1})$$

## 3. Calculation of Bulk Modulus

Bulk modulus  $K$  of PbS NCs were calculated by fitting measure data to Vinet equation of state (EOS):<sup>4,5</sup>

$$P = 3Kv^{-2/3} [1 - v^{1/3}] \exp \left\{ 1.5(K' - 1) [1 - v^{1/3}] \right\} \quad (\text{S2})$$

Where  $v$  is the normalized unit cell volume with respect to the ambient pressure value:  $v(P) = V(P)/V_0 = [a(P)/a_0]^3$ ;  $K$  is the bulk modulus under ambient pressure, and  $K = dK/dP|_{P=0}$  is the pressure derivative of the bulk modulus. In this study,  $K'$  is fixed at 4.0 for fair comparison between samples.<sup>6,7</sup> The Vinet EOS fits of the measured data are presented in Figure S3. The slight deviation of the experimental data from the ideal shape of the EOS is likely to be a result of deviatoric stresses when pressure is high.<sup>8</sup> The variable bulk modulus indicates size-dependence of compressibility of PbS NCs as detailed in the main text.

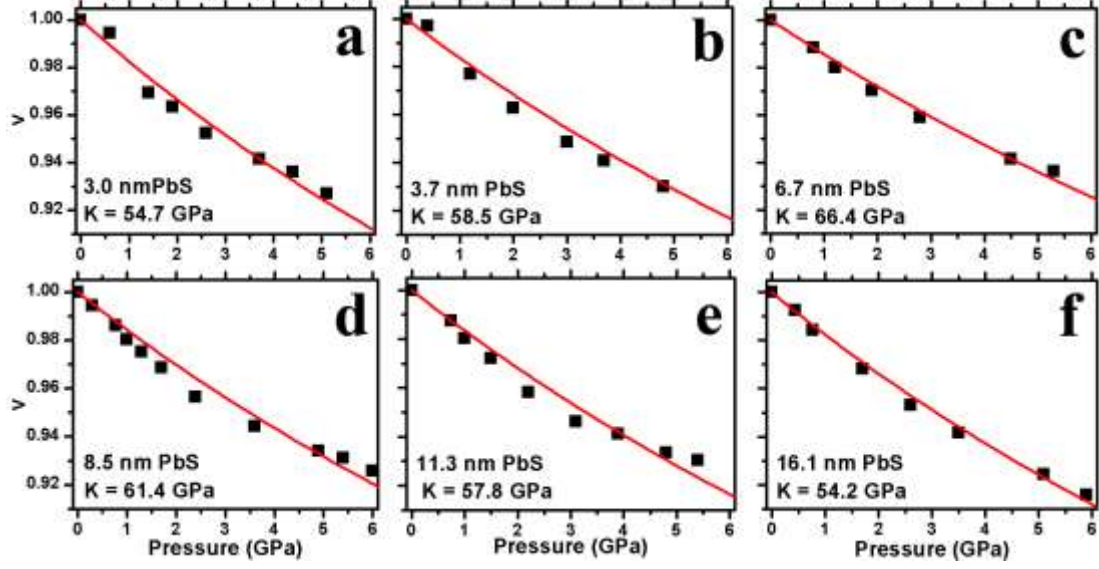


**Figure S3.** Compressibility of (a) 3.0, (b) 3.7, (c) 6.7, (d) 8.5, (e) 11.3 and (f) 16.1 nm PbS NCs. Solid lines are Vinet EOS fits.

#### 4. Lattice Expansion Model

We estimate the influence of atomic lattice expansion on elastic modulus in PbS NCs. The Young's modulus  $Y$  is related to the distance between the nearest-neighboring atoms at equilibrium  $d_{nn}$  by:<sup>9,10</sup>

$$Y = \beta / d_{nn} \quad (\text{S3})$$

where  $\beta$  is a force constant given by

$$\beta = \left. \frac{d^2 u}{dr^2} \right|_{r=d_{nn}} \quad (\text{S4})$$

where  $u$  is the inter-atomic pair potential. When  $u$  is approximated as a Lennard-Jones potential with binding energy  $\varepsilon$ , *i.e.*:

$$u = \varepsilon \left[ \left( \frac{d_{nn}}{r} \right)^{12} - 2 \left( \frac{d_{nn}}{r} \right)^6 \right] \quad (\text{S5})$$

Then we have

$$\beta = \left. \frac{d^2 u}{dr^2} \right|_{r=d_{nn}} = \frac{72\varepsilon}{d_{nn}^2} \quad (\text{S6})$$

And

$$Y = \frac{72\varepsilon}{d_{nn}^3} \quad (S7)$$

The bulk modulus is then given by

$$K = \frac{Y}{3(1-\nu)} = \frac{72\varepsilon}{3(1-\nu)} \frac{1}{d_{nn}^3} \quad (S8)$$

where  $\nu$  is the Poisson ratio. In the rock salt lattice in PbS,  $d_{nn}$  is proportional to lattice constant  $a_0$ . Assuming size-independent binding energy and Poisson ratio, we can simplify eqn. S8 to be

$$K = \frac{\beta'}{a_0^3} \quad (S9)$$

The constant  $\beta'$  can be obtained from the bulk value of lattice constant and bulk modulus. For PbS, we found  $\beta' = 1.10 \times 10^4 \text{ GPa} \cdot \text{\AA}^3$ .

Using eqn. S9, we estimate the lattice expansion effect on bulk modulus in PbS based on measured lattice constants listed in Table 1 of main text. The calculated bulk moduli of PbS NCs of different sizes are plotted in Figure S4 and compared with the experimental values. It shows that considering only the lattice expansion effect results in bulk modulus smaller than bulk value indicating weakened elastic strength in PbS NCs. This is the opposite of what was observed. On the other hand the lattice expansion model does predict the trend that for very small NCs *i.e.*  $K$  decreases as NC size. However, the shift calculated is much smaller than the measured by about an order of magnitude. Consequently we can rule out a major contribution by lattice expansion.

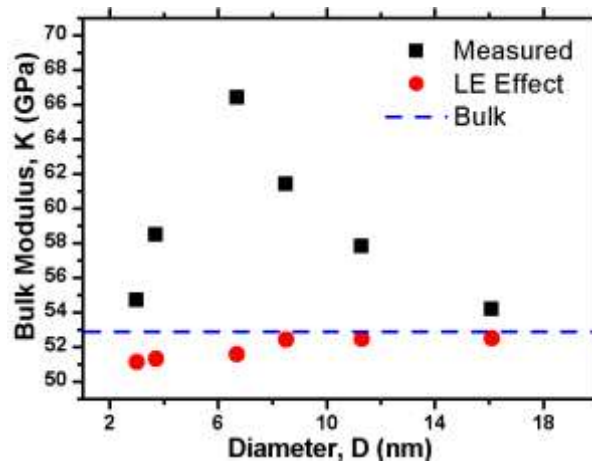


**Figure S4.** Size-dependent bulk modulus caused by lattice expansion (LE) effect (red dots) comparing with measured (black squares) and bulk values (blue dashed line).

## 5. Modeling the Size-Dependent Stiffness in PbS NCs

### a. Details of the Basic Core-Shell Model

The core-shell model is based on a core with a radius of  $R$  and a constant bulk modulus  $K_c$ , which we take to be the value of bulk PbS.<sup>21</sup> On the other hand, the shell contains surface atoms of a skin thickness  $b$  and has a size-dependent bulk modulus  $K_s$  (eqn. 1).  $K_s$  is an apparent stiffness which is expected to be larger than the intrinsic bulk modulus of the shell due to higher packing density at NC surface and pressure shielding effect by the soft ligands.  $K_s$  captures the elasticity of the surface layer, this is expected to vary with the effective curvature of the dot.

$$K_s = K_{s,0} - \frac{k_s}{R^n} \quad (S7)$$

Where  $K_{s,0}$  is the modulus of the surface layer of a flat slab of PbS. Note that  $K_{s,0} \neq K_c$  since the surface atoms packed differently than in the bulk.  $k_s$  and  $n$  are fitted parameters. According to the composite sphere model,<sup>22,23</sup> the effective bulk modulus  $K_{eff}$  which is measured experimentally can be calculated from  $K_s$  and  $K_c$ .<sup>24</sup>

$$K_{eff} = K_s + \frac{c(K_c - K_s)}{1 + (1 - c) \frac{K_c - K_s}{K_s + \frac{4}{3}G_s}} \quad (S8)$$

Where  $c$  is the volume fraction of the core,  $G_s$  is the shear modulus of the surface layer.

$$c = \frac{R^3}{(R + b)^3} \quad (S9)$$

$$G_s = \frac{1 - 2\nu}{2(1 + \nu)} K_s \quad (S10)$$

Where  $\nu = 0.25$  is the Poisson ratio of PbS.

b. *Alternative Effective Stiffness Model*

In addition to the composite sphere model, another effective elastic stiffness adopted from Miller *et. al.*<sup>11</sup> is used to calculate the effective modulus of NCs of different sizes. This is a general model describing the size-dependence of elastic properties:

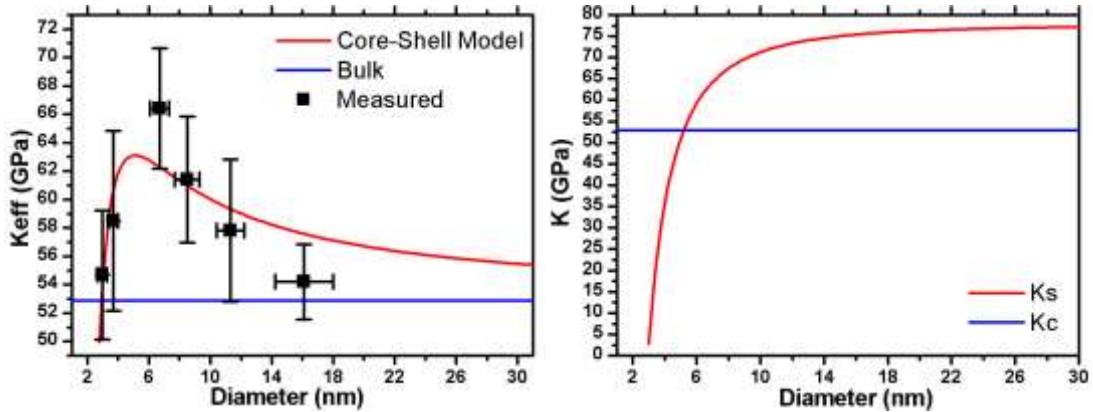
$$\frac{D - D_c}{D_c} = \alpha \frac{S}{E} \frac{1}{h} \quad (\text{S12})$$

Where, the left hand side is deviation of an elastic property  $D$  from that of conventional continuum mechanics  $D_c$ . On the right hand side,  $\alpha$  is a non-dimensional constant that depends on the geometry of the structural element,  $h$  is a characteristic length defining the size of the particle. The quantity  $S$  is a surface elastic property related to the structural element being considered and  $E$  is the corresponding elastic modulus of the bulk material. Note that  $E$  is a positive quantity, but that  $S$  can be positive or negative.

In our case,  $D = K_{eff}$ ,  $D_c = K_{bulk}$ ,  $h$  is the diameter of NC  $d$ ,  $E = K_{bulk}$ ,  $S = K_s$  which size dependent as given by eqn. 1 of main text. And this model now can be rewritten as:

$$K_{eff} = K_{bulk} \left( 1 + \alpha \frac{K_s}{K_{bulk}} \frac{1}{d} \right) \quad (\text{S13})$$

Fitting measured data to this model yields:  $K_{s,bulk} = 78 \text{ GPa}$ ,  $k_s = 169 \text{ GPa} \cdot \text{nm}^2$ ,  $n = 2.0$  and  $\alpha = 1.0$ . Again, as in the composite sphere model, we see  $n = 2$  indicating  $K_s$  scales as the surface area of NC. So it can be written in the form of eqn. 5. And the constant  $\alpha$  happens to be 1 representing the spherical shape of the NCs.





## 6. References

- (1) Hines, M. A.; Scholes, G. D. *Adv. Mater.* **2003**, *15*, 1844.
- (2) Hammersley, A. P. *ESRF Internal Report, ESRF97HA02T* **1997**.
- (3) Holland, T. J. B.; Redfern, S. A. T. *Mineralogical Magazine* **1997**, *61*, 65.
- (4) Bian, K.; Wang, Z.; Hanrath, T. J. *Am. Chem. Soc.* **2012**, *134*, 10787.
- (5) Fei, Y.; Ricolleau, A.; Frank, M.; Mibe, K.; Shen, G.; Prakapenka, V. *Proceedings of the National Academy of Sciences* **2007**, *104*, 9182.
- (6) Podsiadlo, P.; Lee, B.; Prakapenka, V. B.; Krylova, G. V.; Schaller, R. D.; Demortière, A.; Shevchenko, E. V. *Nano Letters* **2011**, *11*, 579.
- (7) Lach-hab, M.; Papaconstantopoulos, D. A.; Mehl, M. J. *J. Phy. Chem. Solids* **2002**, *63*, 833.
- (8) Bassett, W. A. *Journal of Physics: Condensed Matter* **2006**, *18*, S921.
- (9) Nix, W. D.; Gao, H. J. *Acta Metall.* **1998**, *39*, 1653.
- (10) Liang, L. H.; Li, J. C.; Jiang, Q. *Solid State Communications* **2002**, *121*, 453.
- (11) Miller, R. E.; Shenoy, V. B. *Nanotechnology* **2000**, *11*, 139.